Title

Phononic layered composites for stress-wave attenuation

Authors

Nemat-Nasser, S
Sadeghi, H
Amirkhizi, AV
et al.

Publication Date

2015-09-01

DOI

10.1016/j.mechrescom.2015.05.001

Peer reviewed

Phononic Layered Composites for Stress-wave Attenuation

S. Nemat-Nasser[a], H. Sadeghi[a], A. V. Amirkhizi[b], A. Srivastava[c]
[a] Department of Mechanical and Aerospace Engineering, University of California San Diego, CA
[b] Department of Mechanical Engineering, University of Massachusetts Lowell, MA
[c] Department of Mechanical, Materials, and Aerospace Engineering, Illinois Institute of Technology, IL

ABSTRACT

The aim is to design a layered metamaterial with high attenuation coefficient and high in-plane stiffness-to-density ratio using homogenization to calculate and optimize the dynamic effective stiffness and mass density of layered periodic composites (phononic layers) over a broad frequency band. This is achieved by: (1) minimizing the frequency range of the first pass band, (2) maximizing the frequency range of the stop band, and (3) creating local resonance over the second pass band. To verify the theoretical calculation, laboratory samples were fabricated and their attenuation coefficient were measured and compared with the theoretical results. It is observed that over 4 to 20 kHz frequency range the attenuation per unit length in the optimally designed composite can exceed 500 dB/m; which increases with increasing frequency. A dynamic Ashby chart, depicting attenuation coefficient vs. in-plane stiffness-to-density ratio, is presented for various engineering materials and is compared with the fabricated metamaterial to show the significance of our design. This method can be used in variety of applications for stress wave management, e.g., in addition to match the impedance of the resulting composite to that of its surrounding medium to minimize (or essentially eliminate) stress wave reflection.

Keywords: acoustic, metamaterial, sonic, attenuation, filter.

1. INTRODUCTION

With development of various new materials, optimal selection of materials for engineering purposes becomes a challenging task. Standard Ashby charts (Ashby, 2005) have provided designers with a powerful tool to be used as guidance for optimal selection of materials. However, the standard Ashby charts provide information about the quasistatic properties of materials. To address this issue, the concept of dynamic Ashby chart was recently introduced (Nemat-Nasser et al., 2011), seeking to provide frequency dependent properties of materials. Furthermore, an inherent limitation in properties of existing engineering materials is that increase in the attenuation coefficient usually appears at the expense of decrease in their stiffness. For example, polymers have high attenuation coefficient while they have low stiffness; whereas, metals have high stiffness but low attenuation coefficient. Therefore, design and development of stiff materials with high attenuation coefficient, for applications like elastic/acoustic filter where both high stiffness and high attenuation coefficient are needed, is an engineering challenge.

The goal of this study is to use dynamic homogenization (Nemat-Nasser et al., 2011) to calculate the effective stiffness and mass density of layered periodic composites and to design a layered composite with high attenuation coefficient and high in-plane stiffness-to-density ratio. This is achieved by: (1) minimizing the frequency range of the first pass band, (2) maximizing the frequency range of the stop band, and (3) creating local resonance over the second pass band. To verify the theoretical calculation, laboratory samples are fabricated and their attenuation coefficient are measured and compared with the theoretical results. A dynamic Ashby chart, depicting attenuation coefficient vs. in-plane stiffness-to-density ratio, is presented for various engineering materials and is compared with the fabricated sample to show the significance of our design. Here we show it is possible through metamaterial design to create composites that exhibit both high stiffness-to-density ratio and high attenuation at low frequency (a few kHz, corresponding to large wave lengths) using a unit cell size smaller than 2 cm which is not achievable through traditional composite desigh.

Metamaterials are phononic crystals that can be micro-architecturally designed for high stress-wave attenuation (Liu et al., 2000; Ho et al., 2003; Cheng et al., 2008; Huang and Sun, 2009). They have

overall mechanical properties that are not shared by traditional engineering materials (Guenneau et al., 2007; Torrent and Sanchez-Dehesa, 2007; Milton and Willis, 2007; Torrent and Sanchez-Dehesa, 2008). Over certain frequency bands, they may display negative effective density and/or negative effective stiffness. Such extraordinary features are due to local resonance within the composite at certain frequencies. Acoustic metamaterials are highly attenuative near their resonance frequency. Liu et al. (2000) designed a 3-D sonic metamaterial and showed that near the resonance frequencies the metamaterial behaves like a medium with effective negative stiffness. Their experimental results show that at the resonance frequencies the transmission coefficient is very small due to attenuation induced by local resonance. Ho et al. (2003) used several locally resonant materials with different resonance frequencies and showed that each layer vibrates like an independent unit. Their results show significant drop in transmission coefficient at resonance frequencies and they used it to make a broadband sonic shield. Cheng et al. (2008) designed a 1-D ultrasonic metamaterial with both effective density and effective bulk modulus simultaneously negative. They found the transmission coefficient using acoustic transmission line method (ATLM), finite element method, and experimental measurement and observed a substantial drop in transmission spectrum around the resonance frequency. Wang et al. (2004) studied the propagation of longitudinal and transverse elastic waves in locally resonance layered metamaterials. They showed that locally resonant layered periodic composites with lattice constant around a few centimeters can be designed to show stop band at frequencies around a few hundreds of Hertz. Nemat-Nasser and Srivastava (2011) showed that 3-phase layered periodic composites with a heavy central layer and compliant coating embedded in a polymer matrix can be designed to show negative effective density and stiffness over the second pass band. These studies suggest the possibility of using layered metamaterials to design composites with tunable attenuation.

2. THEORY

2.1. Homogenization of layered composites

Nemat-Nasser et al. (2011) developed a homogenization method for calculation of overall elastodynamic properties of layered elastic composites. The dynamic average constitutive relation can be expressed as

$$\bar{\Sigma} = C_{eff}\bar{E}, \quad \bar{P} = \rho_{eff}\dot{\bar{U}} \tag{1}$$

where $\bar{\Sigma}$, $\bar{E}$, $\bar{P}$ and $\dot{\bar{U}}$ are the Bloch-reduced averages of the stress, strain, linear momentum, and velocity, and the barred quantities are defined as

$$\bar{\mathrm{G}} = \frac{1}{d}\int_{-d/2}^{d/2} G(x)dx, \tag{2}$$

where $g(x,t) = G(x)e^{i(kx-\omega t)}$, is any of the field quantities for a plane wave traveling with Bloch wave vector k, and d is the unit cell thickness. C_{eff} and ρ_{eff} are therefore frequency dependent effective stiffness and effective density of the composite. In this paper, we use the transfer matrix method to find the exact field quantities for various Bloch mode shapes and average them for use in eqs. (1) to calculate C_{eff} and ρ_{eff}.

2.2. Wave propagation in layered periodic composites

Consider one unit cell of an infinite layered periodic composite, consisting of N different homogeneous layers as shown in Figure 1. In this Figure, $E^{(j)}, \rho^{(j)}$ and $d^{(j)}$ are the elastic modulus, density and thickness of the j-th layer, respectively. The displacement, u, and stress, σ, at the left boundary of the first layer in the unit cell, x^{1L}, can be related to those at the right boundary of the N-th layer, x^{NR}, by

$$\begin{bmatrix} u(x^{NR}) \\ \sigma(x^{NR}) \end{bmatrix} = \mathbf{T}\begin{bmatrix} u(x^{1L}) \\ \sigma(x^{1L}) \end{bmatrix} \tag{3}$$

where $\mathbf{T} = \mathbf{T}_N\mathbf{T}_{N-1}\ldots\mathbf{T}_1$ is the transfer matrix of the unit cell and $\mathbf{T}_j$ is the transfer matrix of the j-th layer given as

$$\mathbf{T}_j = \begin{bmatrix} \cos(k^{(j)}d^{(j)}) & \sin\left(k^{(j)}d^{(j)}\right)/Z^{(j)} \\ -Z^{(j)}\sin(k^{(j)}d^{(j)}) & \cos(k^{(j)}d^{(j)}) \end{bmatrix}. \tag{4}$$

where $Z^{(j)} = \rho^{(j)} c^{(j)^2} k^{(j)}$, ω is the angular frequency, $k^{(j)}$ is the wave number in the j-th layer, and $c^{(j)}$ is the wave velocity in the j-th layer. For Bloch type waves the stress and displacement at the boundaries of the unit cell are related by

$$\begin{bmatrix} u(x^{NR}) \\ \sigma(x^{NR}) \end{bmatrix} = e^{iQ} \begin{bmatrix} u(x^{1L}) \\ \sigma(x^{1L}) \end{bmatrix} \tag{5}$$

where $Q = kd$ is the normalized Bloch wave number. Combining eqs. (3) and (5) one can find the following eigenvalue problem

$$\mathbf{T}\mathbf{y}(x^{1L}) = e^{iQ}\mathbf{y}(x^{1L}) \tag{6}$$

which may be solved for either ω or Q to find the band structure of a layered periodic composite. In general, the global wave number is a complex number, $k = k_r + ik_i$. Assuming the displacement at the right end of the j-th unit cell is given by $u_j = Ae^{\boldsymbol{i}(k_r+ik_i)x_j}$ and the displacement at the right end of the $j+1$-th unit cell is $u_{j+1} = Ae^{\boldsymbol{i}(k_r+ik_i)(x_j+d)}$, the attenuation per unit thickness in the composite can be expressed as

$$\alpha = -\frac{1}{d}\ln\left(\frac{|u_{j+1}|}{|u_j|}\right) = -\frac{1}{d}\ln\left(\frac{|A\boldsymbol{e}^{\boldsymbol{i}(k_r+ik_i)(x_j+d)}|}{|A\boldsymbol{e}^{\boldsymbol{i}(k_r+ik_i)x_j}|}\right) = -\frac{1}{d}\ln\left(\boldsymbol{e}^{-k_i d}\right) = k_i \tag{7}$$

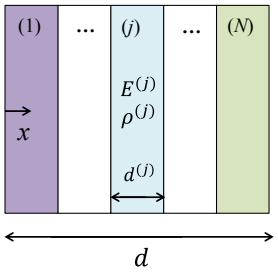

Figure 1. Unit cell of a layered periodic composite.

3. SAMPLE DESIGN AND THEORETICAL CALCULATION

To illustrate the general methodology in concrete terms, we have designed a 3-phase layered PC with a heavy central layer (steel), sandwiched between two soft layers (foam) and embedded in a polymer based matrix (CFRP). To create the final unit cell, optimization is performed to: (1) minimize the frequency range of the first pass band, (2) maximize the frequency range of the stop band, and (3) create local resonance over the second pass band. The objective function for optimization are the frequency window of the first two pass bands together with the first stop band, with the design parameters being the thickness of each layer in the unit cell. To ensure the existence of a resonance over the entire second pass band, the optimization constraint is to keep the effective properties (mass-density and stiffness) negative on the second band. Consequently, the first pass band is shortened, and the first stop band and the second pass band are widened. The resulting composite exhibits high attenuation over a wide range of frequency, starting from the end of the first pass band to the end of the second stop band. To achieve a high in-plane stiffness-to-density ratio, CFRP is used as the matrix material which has high in-plane but lower out-of-plane stiffness necessary to achieve the metamaterial response. Foam is used for the necessary compliant second phase, keeping its volume fraction as low as possible to avoid compromising the overall stiffness of the composite.

3.1 Sample geometry and composition

The sample designed for this study is a 3-phase composite consisting of periodic layers of carbon fiber reinforced polymer (CFRP), polyester foam, and steel. Figure 2(a, b) show a schematic drawing of the unit cell of the composite and a photograph of its cross section. The thicknesses are: $t_1 = 6.35\,mm$, $t_2 = 3.2\,mm$ and $t_3 = 0.5\,mm$ for CFRP, foam, and steel, respectively. The through-thickness longitudinal wave velocity and density of CFRP, polyester foam and steel are: $c_{CFRP} = 1980\,m/s$,

$\rho_{CFRP} = 1530\ kg/m^3, c_{pf} = 230\ m/s,\ \rho_{pf} = 360\ kg/m^3,\ c_{st} = 5130\frac{m}{s},$ and $\rho_{st} = 7820\ kg/m^3,$ respectively.

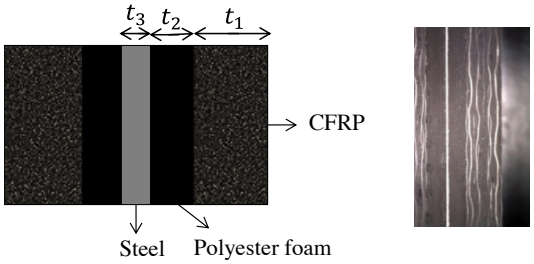

(a) (b)

Figure 2. (a) Unit cell of the designed CFRP/foam/steel periodic composite; and (b) picture of the cross section of the sample.

3.2 Theoretical calculation

Figure 3 (a) shows the theoretical band structure for the CFRP/foam/steel (CFS) sample. In this figure the real part of the normalized wave number represents the dispersion curve of the composite while the imaginary part represents the attenuation. It can be seen that the first pass band ends at 3.9 kHz, followed by a wide stop band and then the second pass band (dissipating band) from 9.2 to 36 kHz.

This band structure is induced by the presence of the heavy central layer steel plate which is sandwiched between two soft foam layers and embedded in a high-in-plane low-out-of-plane stiffness CFRP matrix. With this microstructure it was possible to: (i) move the end of the first pass band to sonic frequency range, (ii) widen the second stop band, and (iii) create a local resonance over the second pass band. Figure 3(b, c) show the effective density and compliance of the composite, respectively. It can be seen that there is a discontinuity in the value of the effective density at 9.1 kHz which is due to presence of a local resonance. Above 3.9 kHz (up to 36 kHz) the attenuation coefficient would be be quite large because of the presence of the stop bands and the local resonance.

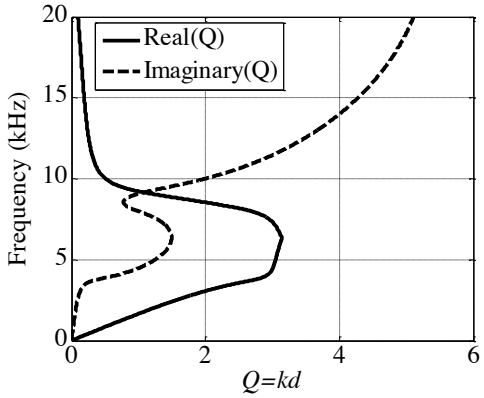

(a)

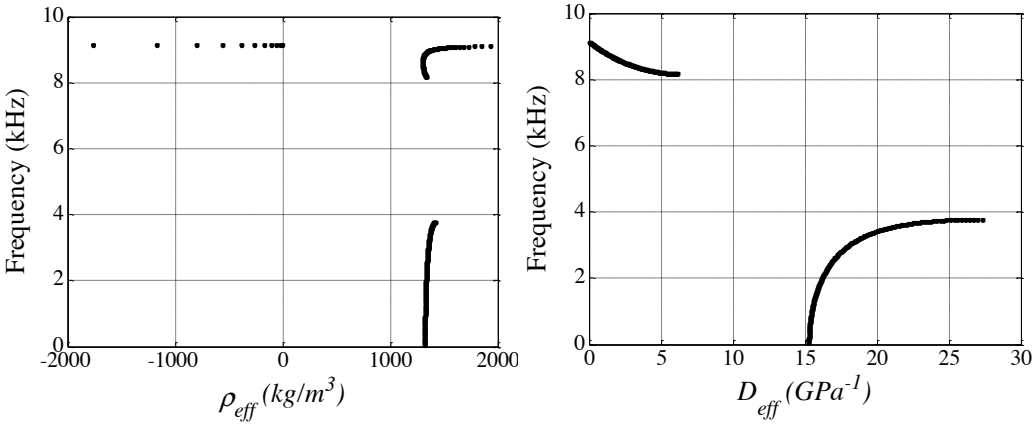

(b) (c)

Figure 3: (a) The band structure, (b) effective density, and (c) effective compliance for the optimally designed CFS (CFRP/foam/steel) composite.

4. EXPERIMENTAL SETUP AND RESULTS

4.1. Experimental setup

A wave packet envelop made of 10 sine waves at the carrier frequency, *f*, multiplied by a half-period of another sinusoidal wave of *1*/20 *f* carrier frequency is generated through a wave generator and is sent to an amplifier (Amirkhizi and Nemat-Nasser, 2011),

$$u(0,t) = Asin(2\pi ft)\sin(2\pi ft/20) \quad \text{where } 0 < t < 10/f \tag{8}$$

The amplified signal is sent to a contact piezoelectric transducer, propagated through the sample, and received by another transducer on the opposite end of the sample. The received transmitted signal is stored by an oscilloscope. Measurements are done from 3 to 20 kHz and data are recorded at every 200 Hz. In order to find the attenuation in the sample, amplitude of the transmitted wave through one unit cell, A_1, and two unit cells, A_2, are measured and used to find the attenuation coefficient in dB/m as

$$\alpha = \frac{20}{d}\log\left(\frac{A_1}{A_2}\right) \tag{9}$$

4.2. Results

Figure 4 (a) shows the normalized transmission through 2 unit cells of the CFS sample. The experimental data are normalized with respect to transmitted amplitude in a transducer-to-transducer test. To show that the high attenuation coefficient in the sample is in fact due to the metamaterial response, the results for three different reference samples are also presented: (i) CF: the sample is made by removing the steel layer from the CFS sample, (ii) CS: the sample is made by removing the foam layers from the CFS sample, and (iii) C: the sample is made of CFRP with the same thickness as the CFS sample. It can be seen that the transmission through the CFS sample is significantly lower than C and CS samples over the entire frequency range. While up to 16 kHz the transmission in CFS and CF samples are close, above 16 kHz the transmission through CFS sample is significantly lower. Figure 4 (b) shows the experimental attenuation per unit length in the CFS sample as a function of frequency. Theoretical attenuation calculated from EQ. (7) is also shown in this figure for comparison. It is seen that the experimental results are in good agreement with the theoretical calculations. Also, it can be observed that above 4 kHz the attenuation per unit length is more than 500 dB/m and increases with increasing frequency. The difference between the theoretical and experimental data in Figure 4 (b) stems mainly from the frequency dependence of the properties of the foam and the polymer components of the composite, and perhaps more significantly, from the sample geometry, i.e., the dispersion due to the cylindrical shape of the sample.

Figure 5 shows a dynamic Ashby chart, depicting attenuation coefficient vs. in-plane stiffness-to-density ratio, for various engineering materials, as well as that from our metamaterial design. Overall static in-plane stiffness-to-density ratio of the CFS sample is calculated using the volume averages. In this figure it can be seen that polymers have high attenuation coefficient but small stiffness-to-density ratio, while metals have high stiffness-to-density ratio with small attenuation coefficient, whereas our metamaterial maintains both a large attenuation coefficient and also a large in-plane stiffness-to-density ratio. This kind of behavior cannot be achieved through any natural material at sonic frequency range. It demonstrates the significance of the current metamaterial design.

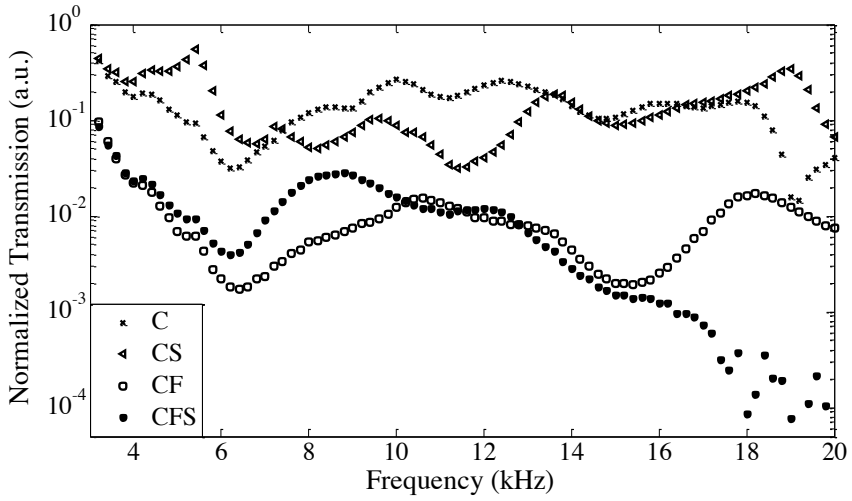

(a)

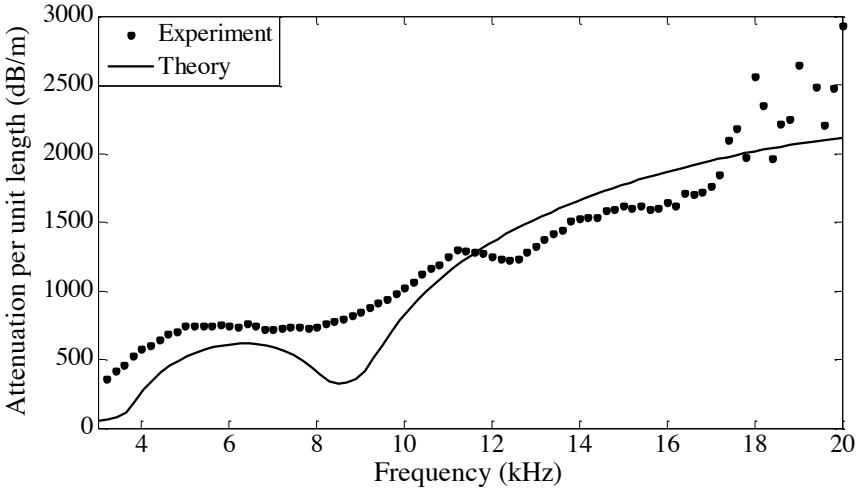

(b)

Figure 4: (a) Normalized experimental transmission for different samples (b) theoretical and experimental attenuation per unit length for CFS (CFRP/foam/steel) sample.

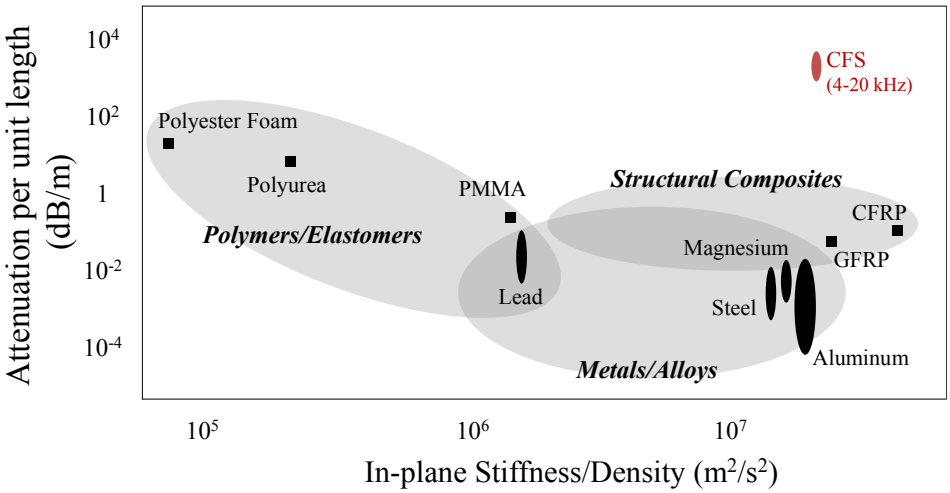

Figure 5: Dynamic Ashby chart for various engineering materials and comparison with optimally designed CFS (CFRP/foam/steel) sample (4-20kHz).

5. CONCLUSION

Dynamic homogenization is used to calculate the effective stiffness and mass density of layered periodic composites and to design a layered composite with high attenuation coefficient and high in-plane stiffness-to-density ratio. This is achieved by: (1) minimizing the frequency range of the first pass band, (2) maximizing the frequency range of the stop band, and (3) creating local resonance over the second pass band. Laboratory samples were fabricated for verification of the theoretical calculation and their attenuation coefficient were measured and compared with the theoretical results. It is observed that over 4 to 20 kHz the attenuation per unit length of the optimally designed composite is more than 500 dB/m and it increases with increasing frequency. A dynamic Ashby chart, depicting attenuation coefficient vs. in-plane stiffness-to-density ratio, is presented for various engineering materials and is compared with the fabricated composite. It is observed that the optimally designed composite exhibits high attenuation coefficient and high in-plane stiffness-to-density ratio which is not achievable through any natural materials. This method can be used in variety of applications for stress wave management.

6. ACKNOWLEDGEMENT

This research has been conducted at the Center of Excellence for Advanced Materials (CEAM) at the University of California, San Diego, under DARPA Grant RDECOM W91CRB-10-1-0006 to the University of California, San Diego.

7. REFERENCES

Amirkhizi, A. V., Nemat-Nasser, S., 2011. Experimental verification of stree-wave bands and negative phase velocity in layered media. Theoretical Applied Mechanics 38, 299-319.

Ashby, M. F., 2005. Materials Selection in Mechanical Design. Third edition, Butterworth-Heinemann, Oxford.

Cheng, Y., Xu, J., Liu, X., 2008. One-dimensional structured ultrasonic metamaterials with simultaneously negative dynamic density and modulus. Physical Review B 77, 045134.

Guenneau, S., Movchan, A., Petursson, G., Ramakrishna, S. A., 2007. Acoustic metamaterials for sound focusing and confinement. New Journal of physics 9, 399.

Ho, K. M., Cheng, C. K., Yang, Z., Zhang, X., Sheng, P., 2003. Broadband locally resonant sonic shields. Applied physics letters 83, 5566-5568.

Huang, H., Sun, C., 2009. Wave attenuation mechanism in an acoustic metamaterial with negative effective mass density. New Journal of Physics 11, 013003.

Liu, Z., Zhang, X., Mao, Y., Zhu, Y., Yang, Z., Chan, C., Sheng, P., 2000. Locally resonant sonic materials. Science 289, 1734-1736.

Milton, G.W., Willis, J.R., 2007. On modifications of Newton's second law and linear continuum elastodynamics. Proceedings of the Royal Society A 463, 855-880.
Nemat-Nasser, S., Srivastava, A., 2011. Negative effective dynamic mass-density and stiffness: Micro-architecture and phononic transport in periodic composites. AIP Advances 1, 041502.
Nemat-Nasser, S., Willis, J., Srivastava, A., Amirkhizi, A., 2011. Homogenization of periodic elastic composites and locally resonant sonic materials. Physical Review B 83, 104103.
Torrent, D., Sanchez-Dehesa, J., 2007. Acoustic metamaterials for new two-dimensional sonic devices. New journal of physics 9, 323.
Torrent, D., Sanchez-Dehesa, J., 2008. Anisotropic mass density by two-dimensional acoustic metamaterials. New journal of physics 10, 023004.
Wang, G., Yu, D., Wen, J., Liu, Y., Wen, X., 2004. One-dimensional phononic crystals with locally resonant structures. Physics Letters A 327, 512-521.